The generalized super-twisting algorithm with adaptive gains

Ida-Louise G. Borlaug and Kristin Y. Pettersen and Jan Tommy Gravdahl

Abstract— **In this paper a novel adaptive generalized super-twisting algorithm is proposed for a class of systems whose perturbations and uncertain control coefficients are time- and state-dependent. The proposed approach uses dynamically adapted control gains, and it is proven that this ensures global finite-time convergence. A non-smooth strict Lyapunov function is used to obtain the conditions for the global finite-time stability. As a case study, it is also shown that the tracking errors of an articulated intervention AUV converge asymptotically to zero when the proposed adaptive generalized super-twisting algorithm is applied. A simulation study is performed that shows the effectiveness of the proposed algorithm.**

I. Introduction

Sliding mode control (SMC) is a robust and versatile nonlinear control approach that is particularly well suited for controlling perturbed control systems. In particular control systems perturbed by matched uncertainties and disturbances [1]. We achieve these properties by using a discontinuous control law. The discontinuous element gives us robustness, but it also introduces chattering, i.e. high frequency switching in the control input. Chattering can be avoided by using a saturation or sigmoid function instead of the discontinuous signum function, [2], [3]. We then achieve a continuous control input, but we restrict our sliding system's trajectories to a boundary around the the sliding surface, loosing the robustness to the disturbances. However, chattering can also be avoided using higher-order sliding mode (HOSM) techniques [4]–[6]. We then achieve a continuous control input, without loosing any robustness. The HOSM methods drive the sliding variable and its derivatives to zero in the presence of disturbances and uncertainties [7].

The super-twisting algorithm (STA) [8] is one of the most powerful second-order continuous SMC algorithm. It attenuates chattering by introducing a dynamic extension to the system such that the discontinuous term is hidden behind an integrator. This is why it generates a smooth continuous control input that drives the sliding variable and its derivatives to zero in finite time in the presence of smooth matched disturbances with bounded gradient. The main drawback of this approach is that the boundaries of the disturbance gradient have to be known. This boundary is not always easily estimated and often that leads to overestimation, which leads to unnecessarily large control gains. Therefore, in [7] a STA with adaptive gains was proposed. The approach continuously drives the sliding variable and its derivatives to zero in the presence of a bounded disturbance with unknown boundary, such that no conservative upper bound on the disturbance gradient has to be considered to maintain sliding, because of the adaptive gains.

In recent years different Lyapunov functions have been designed in order to obtain convergence conditions and estimates of the reaching time. However, these Lyapunov proofs are made under conservative assumptions. The perturbations are dependent only on time [8], [9], the control coefficient is known [8]–[11], or perturbations are dependent on state and time, but it is supposed that their total time derivative, i.e. the control signal, is a priori bounded by some constant [10], [12]. Therefore, [13] proposed a generalized super-twisting algorithm (GSTA) where they consider a more general scenario, i.e. the case when both the perturbations and control coefficients are state- and time-dependent and the control coefficients are uncertain. This approach gives us some additional theoretical properties over the regular STA proposed in [8]. However, we also here have to know the boundaries of the perturbations and control coefficients to obtain bounds on the control gains which are not too conservative.

In this paper we therefore propose an adaptive GSTA for a class of system whose perturbations and uncertain control coefficients are time- and state-dependent, i.e. we combine the best properties of the STA with adaptive gains [7] and the GSTA [13]. The proposed approach consists in using dynamically adapted control gains that ensure global finite-time (GFT) convergence. The advantage with adaptive gains is that no conservative upper bound has to be considered on the perturbations and control coefficients to maintain sliding. We prove that the resulting closed-loop system is globally finite-time stable (GFTS).

In [14] and [15] two alternative adaptive GSTA have been proposed for the GSTA proposed in [16], for SISO and MIMO system, respectively. The approach proposed in this paper differs from these two algorithms, specifically the approach proposed also handles unknown control coefficients. In [17] a third alternative adaptive GSTA has been proposed. The approach proposed in this paper differs from the algorithm in [17], as this also handles state-dependent disturbances, not just time-dependent disturbances. These distinctions are important because it allows us to use the adaptive GSTA to control a larger class of systems, and, in particular, it allows us to control an articulated intervention-AUV (AIAUV) which was our motivation to look into an adaptive GSTA that handles unknown control coefficients and state-dependent disturbances.

The AIAUV is an underwater vehicle with multiple joints and multiple thrusters [18]. The AIAUV is subject to hy-

I.-L. G. Borlaug, K. Y. Pettersen and J. T. Gravdahl are with the Centre for Autonomous Marine Operations and Systems, Department of Engineering Cybernetics, Norwegian University of Science and Technology (NTNU), Trondheim, Norway. {Ida.Louise.Borlaug, Kristin.Y.Pettersen, Tommy.Gravdahl}@ntnu.no

drodynamic and hydrostatic parameter uncertainties, uncertain thruster characteristics, unknown disturbances, unmodeled dynamics and large coupling forces caused by joint motion, and it is therefore essential for the control approach to be robust. We have therefore previously looked into using SMC for trajectory tracking for the AIAUV, since trajectory tracking is essential for the AIAUV to be able to move in confined spaces and to perform intervention tasks. In [19] and [20] we investigated using the STA with adaptive gains to control the AIAUV, and in [21] and [22] we investigated using the GSTA to control the AIAUV. In [23], we have compared the two SMC algorithms both through simulations and experimental results, and we saw that the STA with adaptive gains gave better tracking results than the GSTA, even though the GSTA has better theoretical properties. The adaptive gains are thus seen to be very practical and gives us tuning advantages. We therefore wanted to have the practical advantages from the adaptive gains together with the theoretical advantages of the GSTA, to control the AIAUV. We therefore use the AIAUV as a case study in this paper, to show the effectiveness of the proposed adaptive GSTA. We also show that the adaptive GSTA makes the tracking errors of the AIAUV converge asymptotically to zero.

The contributions of the paper can be summarized as follows. A novel adaptive GSTA is proposed for a class of systems whose perturbations and uncertain control coefficients are time- and state-dependent. The proposed approach consists in using dynamically adapted control gains in a GSTA, which ensures GFT convergence. A non-smooth strict Lyapunov function is used to obtain the conditions for the GFT stability. It is also shown that the adaptive GSTA makes the tracking errors of the AIAUV converge asymptotically to zero. A simulation study is performed to show the effectiveness of the proposed algorithm.

The remainder of the paper is organized as follows. In Sec. II, the problem statement and main results are given. The case study for the AIAUV is given in Sec. III. In Sec. IV, the conclusions and suggestions for future work are given.

II. Problem statement and main results

In this section we will prove that the GSTA with adaptive gains makes the system trajectories globally converge to zero in finite-time while taking into account the unknown bounds of the uncertain control coefficient and perturbation.

A. System dynamics

Consider the dynamic system represented by the differential equation

$$\dot{\sigma} = \gamma(\sigma,t)u + \varphi(\sigma,t) \tag{1}$$

where $\sigma \in \mathbb{R}$ is the state vector, $u \in \mathbb{R}$ is the control input vector. The functions $\gamma(\sigma,t)$ and $\varphi(\sigma,t)$ are uncertain functions dependent on the state and time. By following [13] we make the following assumptions

Assumption 1: The functions $\gamma(\sigma,t)$ and $\varphi(\sigma,t)$ are Lipschitz continuous functions with respect to t and $\gamma(\sigma,t)$, $\varphi(\sigma,t) \in \mathcal{C}^1$ with respect to σ.

Assumption 2: The uncertain control coefficient function is bounded by

$$0 < k_m \leq \gamma(\sigma,t) \leq k_M \tag{2}$$

where k_m and k_M are positive constants.

Assumption 3: The perturbation term $\varphi(\sigma,t)$ can be split into two parts

$$\varphi(\sigma,t) = \varphi_1(\sigma,t) + \varphi_2(\sigma,t) \tag{3}$$

where the first term is vanishing at the origin, i.e. $\varphi_1(0,t) = 0 \ \forall \ t \geq 0$, and bounded by

$$|\varphi_1(\sigma,t)| \leq \alpha|\phi_1(\sigma)|, \qquad \alpha > 0 \tag{4}$$

Assumption 4: The total time derivative of the second-term divided by the control coefficient $\gamma(\sigma,t)$ can be represented as

$$\begin{aligned} \frac{d}{dt}\big(\gamma^{-1}(\sigma,t)\varphi_2(\sigma,t)\big) &= \underbrace{\gamma^{-1}\frac{\partial\varphi_2}{\partial t} - \gamma^{-2}\varphi_2\frac{\partial\gamma}{\partial t}}_{\delta_1(\sigma,t)} + \\ \underbrace{\left(\gamma^{-1}\frac{\partial\varphi_2}{\partial\sigma} - \gamma^{-2}\varphi_2\frac{\partial\gamma}{\partial\sigma}\right)}_{\delta_2(\sigma,t)}\dot{\sigma} &= \delta_1(\sigma,t) + \delta_2(\sigma,t)\dot{\sigma} \end{aligned} \tag{5}$$

where $\delta_1(\sigma,t)$ and $\delta_2(\sigma,t)$ are bounded by positive constants

$$|\delta_1(\sigma,t)| \leq \bar{\delta}_1, \qquad |\delta_2(\sigma,t)| \leq \bar{\delta}_2 \tag{6}$$

B. Generalized super-twisting algorithm with adaptive gains

In this section, the equations describing the adaptive GSTA are presented. The GSTA proposed in [13] can be written as

$$\begin{aligned} u_{\text{GSTA}} &= -k_1\phi_1(\sigma) + z \quad \in \mathbb{R} \\ \dot{z} &= -k_2\phi_2(\sigma) \end{aligned} \tag{7}$$

where

$$\begin{aligned} \phi_1(\sigma) &= \lceil\sigma\rfloor^{\frac{1}{2}} + \beta\sigma \\ \phi_2(\sigma) &= \frac{1}{2}\lceil\sigma\rfloor^0 + \frac{3}{2}\beta\lceil\sigma\rfloor^{\frac{1}{2}} + \beta^2\sigma \end{aligned} \tag{8}$$

where $\lceil a\rfloor^b = |a|^b\,\text{sgn}(a)$, and $k_1 \in \mathbb{R}$, $k_2 \in \mathbb{R}$ and $\beta \in \mathbb{R}$ are controller gains. Motivated by [7] we propose to let k_1 and k_2 be adaptive gains defined by the update law

$$\dot{k}_1 = \begin{cases} \omega_1\sqrt{\frac{\gamma_1}{2}}, & \text{if } \sigma \neq 0 \\ 0, & \text{if } \sigma = 0 \end{cases} \tag{9a}$$

$$k_2 = 2\varepsilon k_1 + \lambda + 4\varepsilon^2 \tag{9b}$$

where $\varepsilon \in \mathbb{R}$, $\lambda \in \mathbb{R}$, $\gamma_1 \in \mathbb{R}$ and $\omega_1 \in \mathbb{R}$ are positive constants.

C. Closed-loop dynamics

The closed-loop dynamics is obtained by inserting (3) and (7) in (1), such that we obtain

$$\dot{\sigma} = -k_1\gamma(\sigma,t)\phi_1(\sigma) + \varphi_1(\sigma,t) + \gamma(\sigma,t)\big(z + \gamma^{-1}(\sigma,t)\varphi_2(\sigma,t)\big) \tag{10}$$

By defining $\sigma_1 = \sigma$ and $\sigma_2 = z + \gamma^{-1}(\sigma_1,t)\varphi_2(\sigma_1,t)$, we can represent the closed-loop dynamics as

$$\dot{\sigma}_1 = \gamma(\sigma_1,t)\big(-k_1\phi_1(\sigma_1) + \gamma^{-1}(\sigma_1,t)\varphi_1(\sigma_1,t) + \sigma_2\big) \tag{11a}$$

$$\dot{\sigma}_2 = -k_2\phi_2(\sigma_1) + \frac{d}{dt}\big(\gamma^{-1}(\sigma_1,t)\varphi_2(\sigma_1,t)\big) \tag{11b}$$

Theorem 1: Suppose that $\gamma(\sigma_1,t)$ and $\varphi(\sigma_1,t)$ in system (1) satisfy Assumptions 1-4. Then, the closed-loop dynamics in (11) is GFTS, such that the states σ_1 and σ_2 converge to zero and z converges to $-\gamma^{-1}(0,t)\varphi_2(0,t)$, globally and in finite time, if the gains k_1 and k_2 are designed as in (9), $\beta>0$, $\lambda>0$, $\omega_1>0$, $\gamma_1>0$ and $\varepsilon=\frac{\omega_2}{2\omega_1}\sqrt{\frac{\gamma_2}{\gamma_1}}$ where $\omega_2>0$ and $\gamma_2>0$.

Remark 1: Note that the proof is for a one-dimensional case, but since SMC approaches do not use model information we can separate the n dimensions into n one-dimensional cases. The proof thus holds for n dimensions as long as Assumptions 1-4 hold for each dimension. This will be demonstrated in the case study in Sec. III.

Proof: From [13] we have that the closed-loop system in (11) is GFTS when constant values of k_1, k_2 and $\beta>0$ are used in (7) and the gains are chosen according to [13, Theorem 2.1]. This is proven using the Lyapunov function candidate

$$V_0=\xi^T P\xi,\quad P=\begin{bmatrix}p_1 & -1\\ -1 & p_2\end{bmatrix} \tag{12}$$

where $p_1p_2>1$ and $\xi^T=\begin{bmatrix}\phi_1(\sigma_1) & \sigma_2\end{bmatrix}$. It is shown that the derivative along the trajectories of the system is

$$\begin{aligned}\dot V_0 &\le -2\gamma(\sigma_1,t)\phi_1'(\sigma_1)\xi^T Q(t)\xi\\ &\le -\mu_1 V_0^{\frac{1}{2}}(\sigma_1,\sigma_2)-\mu_2 V_0(\sigma_1,\sigma_2)\end{aligned} \tag{13}$$

where

$$\mu_1=\frac{k_m\epsilon\lambda_{\min}^{\frac{1}{2}}\{P\}}{\lambda_{\max}\{P\}},\qquad \mu_2=\beta\frac{2k_m\epsilon}{\lambda_{\max}\{P\}} \tag{14}$$

and $Q(t)$ is positive definite if the gains are chosen according to [13, Theorem 2.1]. For the proposed adaptive GSTA, however, k_1 and k_2 are not constants. Instead, k_1 and k_2 are time-varying functions, given by (9). Motivated by [7], we use the Lyapunov function candidate (12), to find a k_1 satisfying (9a) that makes $Q(t)$ positive definite when k_2 is chosen as (9b). From [13] the elements of $Q(t)$ are

$$\begin{aligned}Q(t)&=\begin{bmatrix}q_1(t) & q_2(t)\\ q_2(t) & q_3(t)\end{bmatrix}\\ &=\begin{bmatrix}\tilde k_1\tilde p_1-\tilde k_2 & \frac{1}{2}(p_2\tilde k_2-(\tilde k_1\tilde h+\tilde p_1))\\ \frac{1}{2}(p_2\tilde k_2-(\tilde k_1\tilde h+\tilde p_1)) & \tilde h\end{bmatrix}\end{aligned} \tag{15}$$

where

$$\begin{aligned}\tilde p_1&=\Big(p_1-\frac{\delta_2(\sigma_1,t)}{\phi_1'(\sigma_1)}\Big)\Rightarrow\tilde p_1\in[\underline{p}_1,\bar p_1]=\Big[p_1-\frac{\bar\delta_2}{\beta},p_1+\frac{\bar\delta_2}{\beta}\Big]\\ \tilde k_2&=\gamma^{-1}(\sigma_1,t)\Big(k_2-\frac{\delta_1(\sigma_1,t)}{\phi_2(\sigma_1)}\Big)\Rightarrow\tilde k_2\in[\underline{k}_2,\bar k_2]\\ &=\Big[\frac{1}{k_M}(k_2-2\bar\delta_1),\frac{1}{k_m}(k_2+2\bar\delta_1)\Big]\\ \tilde k_1&=\Big(k_1-\gamma^{-1}(\sigma_1,t)\frac{\varphi_1(\sigma_1,t)}{\phi_1(\sigma_1)}\Big)\Rightarrow\tilde k_1\in[\underline{k}_1,\bar k_1]\\ &=\Big[k_1-\frac{\alpha}{k_m},k_1+\frac{\alpha}{k_m}\Big]\\ \tilde h&=\Big(1-\frac{p_2\delta_2(\sigma_1,t)}{\phi_1'(\sigma_1)}\Big)\Rightarrow\tilde h\in[\underline{h},\bar h]=\Big[1-\frac{p_2\bar\delta_2}{\beta},1+\frac{p_2\bar\delta_2}{\beta}\Big]\end{aligned} \tag{16}$$

If we choose $\tilde k_1=k_1-\frac{\alpha}{k_m}$ and $\tilde k_2=\frac{1}{k_m}(k_2+2\bar\delta_1)$, i.e. such that $Q(t)$ is the most negative, we can rewrite $Q(t)$ as

$$Q(t)=\begin{bmatrix}(k_1-\frac{\alpha}{k_m})\tilde p_1-\frac{1}{k_m}(k_2+2\bar\delta_1) & q_2(t)\\ \frac{1}{2}\Big(\frac{p_2}{k_m}(k_2+2\bar\delta_1)-\big((k_1-\frac{\alpha}{k_m})\tilde h+\tilde p_1\big)\Big) & \tilde h\end{bmatrix} \tag{17}$$

For the matrix $Q(t)$ in (17) to be positive definite we need $q_1(t)>0$ and $\det(Q(t))>0$. By using k_2 as in (9b) and calculating the determinant of $Q(t)$ in (17) we obtain

$$\begin{aligned}&\det(Q(t))=q_1(t)q_3(t)-q_2^2(t)\\ &=\Big((k_1-\frac{\alpha}{k_m})\tilde p_1-\frac{1}{k_m}\Big(2\varepsilon k_1+\lambda+4\varepsilon^2+2\bar\delta_1\Big)\Big)\tilde h\\ &-\frac{1}{4}\Big(\frac{p_2}{k_m}\Big(2\varepsilon k_1+\lambda+4\varepsilon^2+2\bar\delta_1\Big)-\Big((k_1-\frac{\alpha}{k_m})\tilde h+\tilde p_1\Big)\Big)^2\\ &=\tilde h\tilde p_1k_1-\frac{\alpha\tilde h\tilde p_1}{k_m}-\frac{2\varepsilon\tilde h}{k_m}k_1-\frac{\lambda\tilde h}{k_m}-\frac{4\varepsilon^2\tilde h}{k_m}-\frac{2\bar\delta_1\tilde h}{k_m}\\ &-\frac{1}{4}\Big(\frac{2\varepsilon p_2}{k_m}k_1+\frac{\lambda p_2}{k_m}+\frac{4\varepsilon^2p_2}{k_m}+\frac{2\bar\delta_1p_2}{k_m}-\tilde hk_1+\frac{\alpha\tilde h}{k_m}-\tilde p_1\Big)^2\end{aligned} \tag{18}$$

By introducing $k_a=\frac{\alpha\tilde h\tilde p_1}{k_m}+\frac{\lambda\tilde h}{k_m}+\frac{4\varepsilon^2\tilde h}{k_m}+\frac{2\bar\delta_1\tilde h}{k_m}>0$ and $k_b=\frac{\lambda p_2}{k_m}+\frac{4\varepsilon^2p_2}{k_m}+\frac{2\bar\delta_1p_2}{k_m}+\frac{\alpha\tilde h}{k_m}>0$ we can rewrite (18) as

$$\begin{aligned}&\det(Q(t))=\Big(\Big(\tilde h\tilde p_1-\frac{2\varepsilon\tilde h}{k_m}\Big)k_1-k_a\Big)-\frac{1}{4}\Big(\Big(\frac{2\varepsilon p_2}{k_m}-\tilde h\Big)k_1\\ &+k_b-\tilde p_1\Big)^2=\Big(\Big(\tilde h\tilde p_1-\frac{2\varepsilon\tilde h}{k_m}\Big)k_1-k_a\Big)-\Big(\Big(\frac{\varepsilon^2p_2^2}{k_m^2}-\frac{\varepsilon\tilde hp_2}{k_m}\\ &+\frac{1}{4}\tilde h^2\Big)k_1^2+\Big(\frac{\varepsilon k_bp_2}{k_m}-\frac{\varepsilon\tilde p_1p_2}{k_m}-\frac{1}{2}\tilde hk_b+\frac{1}{2}\tilde h\tilde p_1\Big)k_1\\ &+\frac{1}{4}k_b^2-\frac{1}{2}k_b\tilde p_1+\frac{1}{4}\tilde p_1^2\Big)=\Big(-\frac{\varepsilon^2p_2^2}{k_m^2}+\frac{\varepsilon\tilde hp_2}{k_m}-\frac{1}{4}\tilde h^2\Big)k_1^2\\ &+\Big(\tilde h\tilde p_1-\frac{2\varepsilon\tilde h}{k_m}-\frac{\varepsilon k_bp_2}{k_m}+\frac{\varepsilon\tilde p_1p_2}{k_m}+\frac{1}{2}\tilde hk_b-\frac{1}{2}\tilde h\tilde p_1\Big)k_1-\frac{1}{4}k_b^2\\ &+\frac{1}{2}k_b\tilde p_1-\frac{1}{4}\tilde p_1^2-k_a=(k_d-k_c)k_1^2+(k_e-k_f)k_1+k_h-k_g\end{aligned} \tag{19}$$

where

$$k_c=\frac{\varepsilon^2p_2^2}{k_m^2}+\frac{1}{4}\tilde h^2>0 \tag{20a}$$

$$k_d=\frac{\varepsilon\tilde hp_2}{k_m}>0 \tag{20b}$$

$$k_e=\tilde h\tilde p_1+\frac{\varepsilon\tilde p_1p_2}{k_m}+\frac{1}{2}\tilde hk_b>0 \tag{20c}$$

$$k_f=\frac{2\varepsilon\tilde h}{k_m}+\frac{\varepsilon k_bp_2}{k_m}+\frac{1}{2}\tilde h\tilde p_1>0 \tag{20d}$$

$$k_g=\frac{1}{4}k_b^2+\frac{1}{4}\tilde p_1^2+k_a>0 \tag{20e}$$

$$k_h=\frac{1}{2}k_b\tilde p_1>0 \tag{20f}$$

A solution to

$$\det(Q(t))=(k_d-k_c)k_1^2+(k_e-k_f)k_1+k_h-k_g>0 \tag{21}$$

is then

$$k_1>\frac{k_g-k_h}{k_e-k_f} \tag{22}$$

where we must choose p_1 and p_2 such that $k_f < k_e$ and $k_d = k_c$. To ensure that $k_d = k_c$, we choose

$$p_2 = \frac{\tilde{h}k_m}{2\varepsilon} \tag{23}$$

By inserting (23), in (20a) and (20b) we obtain

$$\begin{aligned} k_c &= \frac{\varepsilon^2(\frac{\tilde{h}k_m}{2\varepsilon})^2}{k_m^2} + \frac{1}{4}\tilde{h}^2 = \frac{1}{2}\tilde{h}^2 \\ k_d &= \frac{\varepsilon\tilde{h}\frac{\tilde{h}k_m}{2\varepsilon}}{k_m} = \frac{1}{2}\tilde{h}^2 \end{aligned} \tag{24}$$

which means that $k_d = k_c$ is ensured. To ensure that $k_f < k_e$, we calculate

$$\begin{aligned} k_f &< k_e \\ \frac{2\varepsilon\tilde{h}}{k_m} + \frac{\varepsilon k_b p_2}{k_m} + \frac{1}{2}\tilde{h}\tilde{p}_1 &< \tilde{h}\tilde{p}_1 + \frac{\varepsilon\tilde{p}_1 p_2}{k_m} + \frac{1}{2}\tilde{h}k_b \end{aligned} \tag{25}$$

By inserting (23) in (25) we obtain

$$\begin{aligned} \frac{2\varepsilon\tilde{h}}{k_m} + \frac{\varepsilon k_b}{k_m}\frac{\tilde{h}k_m}{2\varepsilon} + \frac{1}{2}\tilde{h}\tilde{p}_1 &< \tilde{h}\tilde{p}_1 + \frac{\varepsilon\tilde{p}_1}{k_m}\frac{\tilde{h}k_m}{2\varepsilon} + \frac{1}{2}\tilde{h}k_b \\ \frac{2\varepsilon\tilde{h}}{k_m} + \frac{\tilde{h}k_b}{2} + \frac{1}{2}\tilde{h}\tilde{p}_1 &< \tilde{h}\tilde{p}_1 + \frac{\tilde{h}\tilde{p}_1}{2} + \frac{1}{2}\tilde{h}k_b \\ \frac{2\varepsilon}{k_m} &< \tilde{p}_1 \end{aligned} \tag{26}$$

This means that by choosing $\tilde{p}_1 > \frac{2\varepsilon}{k_m}$ or

$$p_1 > \frac{2\varepsilon}{k_m} + \frac{\bar{\delta}_2}{\beta} \tag{27}$$

we ensure $k_f < k_e$. So by choosing k_1 as in (22), p_1 as in (27) and p_2 as in (23) we obtain $\det(Q(t)) > 0$. Now, to ensure $q_1(t) > 0$ we calculate

$$\begin{aligned} q_1(t) &> 0 \\ \Big(k_1 - \frac{\alpha}{k_m}\Big)\tilde{p}_1 - \frac{1}{k_m}(2\varepsilon k_1 + \lambda + 4\varepsilon^2 + 2\bar{\delta}_1) &> 0 \\ \Big(\tilde{p}_1 - \frac{2\varepsilon}{k_m}\Big)k_1 - \frac{\alpha}{k_m}\tilde{p}_1 - \frac{1}{k_m}(\lambda + 4\varepsilon^2 + 2\bar{\delta}_1) &> 0 \end{aligned} \tag{28}$$

By choosing

$$k_1 > k_q = \Big(\tilde{p}_1 - \frac{2\varepsilon}{k_m}\Big)^{-1}\Big(\frac{\alpha}{k_m}\tilde{p}_1 + \frac{1}{k_m}(\lambda + 4\varepsilon^2 + 2\bar{\delta}_1)\Big) \tag{29}$$

we can ensure that $q_1(t) > 0$. By combining (22) and (29), we obtain

$$k_1 > \frac{k_g}{k_e - k_f} + k_q \tag{30}$$

which will ensure that both $\det(Q(t)) > 0$ and that $q_1(t) > 0$. Note that $-k_h$ is removed compared to (22) since if $k_h > k_g$ that could have made $q_1(t) < 0$. Also note that this does not effect $\det(Q(t)) > 0$ since $\frac{k_g}{k_e - k_f} > \frac{k_g - k_h}{k_e - k_f}$ since $k_h > 0$. By this we can conclude that if k_1 is chosen as in (30), p_1 as in (27) and p_2 as in (23) then the matrix $Q(t)$ will be positive definite, which ensures that the closed-loop system in (11) is GFTS when constant gains are used, i.e. we have proven that there exist a gain k_1 that makes $Q(t)$ positive definite. We now have to prove that by using the adaptive gains as in (9) k_1 will converge such that (30) is satisfied.

Now, we will prove by using the Lypaunov function candidate

$$V = V_0 + \frac{1}{2\gamma_1}(k_1 - k_1^\star)^2 + \frac{1}{2\gamma_2}(k_2 - k_2^\star)^2 \tag{31}$$

where $k_1^\star > 0$ and $k_2^\star > 0$ are constants, that the closed-loop dynamics in (11) is also GFTS with the adaptive gains as in (9). By taking the derivative of (31) we obtain

$$\dot{V} = \dot{V}_0 + \frac{1}{\gamma_1}(k_1 - k_1^\star)\dot{k}_1 + \frac{1}{\gamma_2}(k_2 - k_2^\star)\dot{k}_2 \tag{32}$$

By using that $\dot{V}_0 \leq -\mu_1 V_0^{\frac{1}{2}}(\sigma_1, \sigma_2)$ and subtracting and adding $\frac{\omega_1}{\sqrt{2\gamma_1}}|k_1 - k_1^\star| + \frac{\omega_2}{\sqrt{2\gamma_2}}|k_2 - k_2^\star|$ we can rewrite (32) to be

$$\begin{aligned} \dot{V} \leq& -\mu_1 V_0^{\frac{1}{2}} - \frac{\omega_1}{\sqrt{2\gamma_1}}|k_1 - k_1^\star| - \frac{\omega_2}{\sqrt{2\gamma_2}}|k_2 - k_2^\star| \\ &+ \frac{1}{\gamma_1}(k_1 - k_1^\star)\dot{k}_1 + \frac{1}{\gamma_2}(k_2 - k_2^\star)\dot{k}_2 \\ &+ \frac{\omega_1}{\sqrt{2\gamma_1}}|k_1 - k_1^\star| + \frac{\omega_2}{\sqrt{2\gamma_2}}|k_2 - k_2^\star| \end{aligned} \tag{33}$$

By using the well known inequality

$$(x^2 + y^2 + z^2)^{1/2} \leq |x| + |y| + |z| \tag{34}$$

on (31) we obtain

$$\begin{aligned} \sqrt{V} &= \Big(V_0 + \frac{1}{2\gamma_1}(k_1 - k_1^\star)^2 + \frac{1}{2\gamma_2}(k_2 - k_2^\star)^2\Big)^{\frac{1}{2}} \\ &\leq V_0^{\frac{1}{2}} + \frac{1}{\sqrt{2\gamma_1}}|k_1 - k_1^\star| + \frac{1}{\sqrt{2\gamma_2}}|k_2 - k_2^\star| \end{aligned} \tag{35}$$

We can then derive

$$-\mu_1 V_0^{\frac{1}{2}} - \frac{\omega_1}{\sqrt{2\gamma_1}}|k_1 - k_1^\star| - \frac{\omega_2}{\sqrt{2\gamma_2}}|k_2 - k_2^\star| \leq -\eta\sqrt{V} \tag{36}$$

where $\eta = \min(\mu_1, \omega_1, \omega_2)$. Taking into account (36) we can rewrite (33) as

$$\begin{aligned} \dot{V} \leq& -\eta V^{\frac{1}{2}} + \frac{1}{\gamma_1}(k_1 - k_1^\star)\dot{k}_1 + \frac{1}{\gamma_2}(k_2 - k_2^\star)\dot{k}_2 \\ &+ \frac{\omega_1}{\sqrt{2\gamma_1}}|k_1 - k_1^\star| + \frac{\omega_2}{\sqrt{2\gamma_2}}|k_2 - k_2^\star| \end{aligned} \tag{37}$$

By [7, Proposition 1] we have that the adaptation law (9) makes the adaptive gains k_1 and k_2 bounded. Then there exist positive constants $k_1^\star$ and $k_2^\star$ that make

$$k_1(t) - k_1^\star < 0, \qquad k_2(t) - k_2^\star < 0 \qquad \forall t \geq 0. \tag{38}$$

We can therefore reduce (37) to

$$\begin{aligned} \dot{V} \leq& -\eta V^{\frac{1}{2}} - |k_1 - k_1^\star|\Big(\frac{1}{\gamma_1}\dot{k}_1 - \frac{\omega_1}{\sqrt{2\gamma_1}}\Big) \\ &- |k_2 - k_2^\star|\Big(\frac{1}{\gamma_2}\dot{k}_2 - \frac{\omega_2}{\sqrt{2\gamma_2}}\Big) \end{aligned} \tag{39}$$

where we have to ensure that

$$-|k_1 - k_1^\star|\Big(\frac{1}{\gamma_1}\dot{k}_1 - \frac{\omega_1}{\sqrt{2\gamma_1}}\Big) - |k_2 - k_2^\star|\Big(\frac{1}{\gamma_2}\dot{k}_2 - \frac{\omega_2}{\sqrt{2\gamma_2}}\Big) = 0 \tag{40}$$

to achieve finite-time convergence. That (40) hold is supposed to be achieved through the adaptation of the gains k_1

and k_2, i.e.

$$\dot{k}_1 = \omega_1 \sqrt{\frac{\gamma_1}{2}} \tag{41a}$$

$$\dot{k}_2 = \omega_2 \sqrt{\frac{\gamma_2}{2}} \tag{41b}$$

If we select $\varepsilon = \frac{\omega_2}{2\omega_1}\sqrt{\frac{\gamma_2}{\gamma_1}}$, (9b) and (41b) are equal, since

$$\begin{aligned} &k_2 = 2\varepsilon k_1 + \lambda + 4\varepsilon^2 \quad \Rightarrow \\ &\dot{k}_2 = 2\varepsilon \dot{k}_1 \quad \Rightarrow \quad \dot{k}_2 = \varepsilon\omega_1\sqrt{2\gamma_1} = \omega_2\sqrt{\frac{\gamma_2}{2}} \end{aligned} \tag{42}$$

For the finite-time convergence, $k_1(t)$ must satisfy (30). It means that $k_1(t)$ has to increase in accordance with (41a) until (30) is satisfied, since $k_1(t)$ increases linearly (30) will be met in finite time. That guarantees the positive definiteness of the matrix $Q(t)$. After (30) is satisfied, the finite-time convergence is guaranteed according to (39), and as nicely described in the Introduction of [24] this implies that the closed-loop system in (11) is GFTS. ■

III. Case study: Articulated Intervention AUV

In this section we will apply the theoretical results of Sec. II for tracking control of an AIAUV as a case study to show the effectiveness of the proposed control algorithm. The tracking control problem is similar to [21] where the GSTA without adaptive gains was used. For completeness, the model of the AIAUV and tracking problem are briefly described also here, but for more details please see [21].

A. Modelling and the tracking control problem

In this section, we present the model and the mathematical definition of the tracking control problem for the AIAUV. The AIAUV has n links and $n-1$ motorized joints, where each joint is regarded as a one-dimensional Euclidean joint. The AIAUV also has m thrusters. The AIAUV is modelled as an underwater vehicle-manipulator system, with dynamic equations given in matrix form as [25], [26]

$$\begin{aligned} \dot{\xi} &= J(p)\zeta = \begin{bmatrix} R_B^I(p) & 0_{3\times 3} & 0_{3\times(n-1)} \\ 0_{4\times 3} & J_{k,oq}(p) & 0_{4\times(n-1)} \\ 0_{(n-1)\times 3} & 0_{(n-1)\times 3} & I_{(n-1)\times(n-1)} \end{bmatrix}\zeta \\ M(q)\dot{\zeta} &+ C(q,\zeta)\zeta + D(q,\zeta)\zeta + g(q,R_B^I) = \tau(q) \end{aligned} \tag{43}$$

where $\xi = [\eta_1^T \quad p^T \quad q^T]^T \in \mathbb{R}^{7+(n-1)}$, $\eta_1 = [x \quad y \quad z]^T \in \mathbb{R}^3$ is the position of the base and $p = [\varepsilon^T \quad \eta]^T = [\varepsilon_1 \quad \varepsilon_2 \quad \varepsilon_3 \quad \eta]^T \in \mathbb{R}^4$ is the unit quaternion describing the orientation of the base in the inertial frame and $q \in \mathbb{R}^{(n-1)}$ is the vector representing the joint angles. The rotation matrix R_I^B expresses the transformation from the inertial frame to the body-fixed frame, $J_{k,oq} = \frac{1}{2}[\eta I_3 + S(\varepsilon) \quad -\varepsilon^T]^T$, I_n is the $(n\times n)$ identity matrix, $S(\cdot)$ is the cross-product operator defined as in [27, Definition 2.2], $\zeta = [v^T \quad \omega^T \quad \dot{q}^T]^T \in \mathbb{R}^{6+(n-1)}$, v and ω are the body-fixed linear and angular velocities of the base of the AIAUV, and $\dot{q}$ is the vector of joint angle velocities, $M(q)$ is the inertia matrix including added mass terms, $C(q,\zeta)$ is the Coriolis-centripetal matrix, $D(q,\zeta)$ is the damping matrix and $g(q,R_B^I)$ is the matrix of gravitational and buoyancy forces. The control input is given by the generalized forces $\tau(q)$:

$$\tau(q) = \begin{bmatrix} T(q) & 0_{6\times(n-1)} \\ 0_{(n-1)\times m} & I_{(n-1)\times(n-1)} \end{bmatrix}\begin{bmatrix} \tau_{thr} \\ \tau_q \end{bmatrix} \tag{44}$$

where $T(q) \in \mathbb{R}^{6\times m}$ is the thruster configuration matrix, $\tau_{thr} \in \mathbb{R}^m$ is the vector of thruster forces and $\tau_q \in \mathbb{R}^{(n-1)}$ represents the joint torques. The desired velocities are denoted as $\zeta_d = [v_d^T \quad \omega_d^T \quad \dot{q}_d^T]^T$ in the body-fixed frame, and the desired trajectories are denoted as $\xi_d = [\eta_{1,d}^T \quad p_d^T \quad q_d^T]^T$. The tracking errors then consist of the position error $\tilde{\eta}_1$, the orientation error $\tilde{\varepsilon}$ and the joint angle error $\tilde{q}$, and the tracking error vector can then be written as

$$\tilde{\xi} = \begin{bmatrix} \tilde{\eta}_1 \\ \tilde{\varepsilon} \\ \tilde{q} \end{bmatrix} = \begin{bmatrix} \eta_1 - \eta_{1,d} \\ \eta\varepsilon_d - \eta_d\varepsilon + S(\varepsilon_d)\varepsilon \\ q - q_d \end{bmatrix} \tag{45}$$

The goal of the tracking problem is to make the error vector, $\tilde{\xi}$, converge to zero. The tracking control objective is therefore to make $(\tilde{\xi},\tilde{\zeta}) = (0,0)$, where $\tilde{\zeta} = \zeta - \zeta_d$, an asymptotically stable equilibrium point of (43), which will ensure that the tracking error will converge to zero. Note that for $\tilde{p}$ the tracking control objective is to make $\tilde{p} = \begin{bmatrix} 0_{1\times 3} & \pm 1 \end{bmatrix}^T$ an asymptotically stable equilibrium point. Note that $\tilde{\eta}$ is not included as an independent state in (45), since $\tilde{\eta}$ and $\tilde{\varepsilon}$ satisfy $\eta^2 + \varepsilon^T\varepsilon = 1$. When $\tilde{\varepsilon} \to 0$, then $\tilde{p} = \begin{bmatrix} 0_{1\times 3} & \pm 1 \end{bmatrix}^T$.

B. Adaptive GSTA for the AIAUV

In this section, we develop a tracking control law for the AIAUV based on the adaptive GSTA and show that the tracking errors asymptotically converge to zero. The following theorem establishes the convergence properties of the proposed control law.

Theorem 2: Define the virtual reference vector $\zeta_r = \zeta_d - \Lambda\tilde{\xi}$, with $\Lambda = \mathrm{diag}([\mathrm{K_p R_I^B(p)} \quad \mathrm{sgn}(\tilde{\eta})\mathrm{I_3} \quad \mathrm{K_q}])$, where $\tilde{\eta} = \eta\eta_d + \varepsilon^T\varepsilon_d$ and K_p and K_q are constant, positive definite gain matrices. Let the sliding surface be defined as

$$\sigma = \zeta - \zeta_r \quad \in \mathbb{R}^{6+(n-1)} \tag{46}$$

and let the control input be given by

$$\tau(q) = u_{\mathrm{GSTA}} \quad \in \mathbb{R}^{6+(n-1)} \tag{47}$$

where u_{GSTA} is given in (7)-(9). Then, the sliding surface, $\sigma = 0$, is a GFTS equilibrium point, which then ensures asymptotic convergence of the tracking errors $\tilde{\xi}$.

Proof: By differentiating (46), we obtain

$$\dot{\sigma} = \dot{\zeta} - \dot{\zeta}_r = M^{-1}(\cdot)(-C(\cdot)\zeta - D(\cdot)\zeta - g(\cdot) + \tau(\cdot)) - \dot{\zeta}_r \tag{48}$$

and by using that $\zeta = \sigma + \zeta_r$, we obtain

$$\dot{\sigma} = M^{-1}(\cdot)(-C(\cdot)(\sigma+\zeta_r) - D(\cdot)(\sigma+\zeta_r) - g(\cdot) + \tau(\cdot)) - \dot{\zeta}_r \tag{49}$$

Now, by introducing $\Phi(\sigma,t) = \Phi_1(\sigma,t) + \Phi_2(\sigma,t)$, where $\Phi_1(\sigma,t) = M^{-1}(\cdot)(-C(\cdot)\sigma - D(\cdot)\sigma)$ and $\Phi_2(\sigma,t) = M^{-1}(\cdot)(-C(\cdot)\zeta_r - D(\cdot)\zeta_r - g(\cdot) - M(\cdot)\dot{\zeta}_r)$ and substituting $\tau(\cdot)$ by (47) and (7)-(9), we obtain

$$\dot{\sigma} = -k_1 M^{-1}(\cdot)\phi_1(\sigma) + \Phi_1(\sigma,t) + M^{-1}(\cdot)(z + M(\cdot)\Phi_2(\sigma,t)) \tag{50}$$

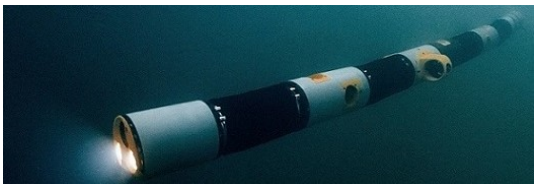

Fig. 1: The Eelume vehicle (Courtesy: Eelume)

Note that $\Phi_1(0,t)=0$. Now by defining $\sigma_1=\sigma$ and $\sigma_2 = z + M(\cdot)\Phi_2(\sigma,t)$, we can write the dynamics as

$$\begin{aligned}\dot{\sigma}_1 &= -k_1 M^{-1}(\cdot)\phi_1(\sigma_1) + \Phi_1(\sigma_1,t) + M^{-1}(\cdot)\sigma_2 \\ \dot{\sigma}_2 &= -k_2\phi_2(\sigma_1) + \frac{d}{dt}\big(M(\cdot)\Phi_2(\sigma_1,t)\big)\end{aligned} \tag{51}$$

Note that (51) is a special case of the form considered in [21, Theorem 2], and therefore $M^{-1}(\cdot)$, $\Phi_1(\cdot)$ and $\Phi_2(\cdot)$ will satisfy Assumptions 1-4 by [21, Theorem 2]. The conditions of Theorem 1 are thus satisfied in each dimension, and thus by Theorem 1 the dynamics in (51) is GFTS. The sliding surface $\sigma=0$ is therefore a GFTS surface, which means that σ converges to zero in finite time.

Once the system trajectories are confined to $\sigma=0$, the tracking error dynamics are given by

$$\tilde{v} = -K_p R_I^B(p)\tilde{\eta}_1 \tag{52a}$$

$$\zeta - \zeta_d = -\Lambda\tilde{\xi} \quad \Leftrightarrow \quad \tilde{\omega} = -\operatorname{sgn}(\tilde{\eta})\tilde{\varepsilon} \tag{52b}$$

$$\dot{\tilde{q}} = -K_q\tilde{q} \tag{52c}$$

For the position error (52a) it is proven in [28] that the equilibrium point $\tilde{\eta}_1$ is UGAS, and for the orientation error (52b) it is proven in [28] that there are two uniformly asymptotically stable equilibrium points, $[\tilde{\varepsilon},\tilde{\eta}]=[0,\pm1]$, both representing perfect alignment between the desired and the actual orientation of the AIAUV. Finally, (52c), shows that the joint angle errors, $\tilde{q}$, converge uniformly globally exponentially to zero, since K_q is chosen positive definite. ■

C. Simulation results

In this section the implementation, simulation set-up and simulation results will be presented.

1) Implementation: The complete model and controllers are implemented in MATLAB Simulink. The model is implemented by the method described in [29], and is based on the Eelume robot, Fig. 1. The AIAUV has $n=9$ links, $n-1=8$ revolute joint and $m=7$ thrusters. The AIAUV has the same link and joint properties as in [21]. To create a continuous trajectory for the AIAUV to follow, we use a filter to generate a continuous trajectory between setpoints. The thruster allocation matrix is implemented as proposed in [18]. For implementation purposes, a small boundary is put on σ so the adaptive gains can be expressed as

$$\dot{k}_1 = \begin{cases}\omega_1\sqrt{\frac{\gamma_1}{2}}, & \text{if } |\sigma| > \alpha_m \\ 0, & \text{if } |\sigma| \le \alpha_m\end{cases} \tag{53a}$$

$$k_2 = 2\varepsilon k_1 + \lambda + 4\varepsilon^2 \tag{53b}$$

where the design parameter $\alpha_m \in \mathbb{R}^{6+(n-1)}$ is a small positive constant chosen empirically. This is done since numerically σ will never be exactly zero.

2) Simulations: The simulation case chosen highlights the two different modes, transport mode and operation mode, which are explained in detail in [18]. Transport mode is for long-distance travel, and operation mode is for performing inspections and intervention tasks. In this case we start in transport mode, i.e. start with the robot in an I-shape (all the joint angles are equal to zero: $q=0\,\text{deg}$), moving forward in the x-direction and downward in the z-direction, before moving into operation mode at 80s. In operation mode we perform an inspection, by setting the AIAUV in C-shape (every second joint angle is equal to $45\,\text{deg}$), and then moving joint 7 and 8 in a circular motion such that link 9 is moving around, performing an inspection. For the simulations, a fixed-step solver with a step size of 10^{-4} was used. The gains were chosen as: $\beta_{\text{GSTA}} = [80e_{14}]^T$, $\lambda = [0.1e_6 \quad 10e_8]^T$, $\varepsilon_1 = \frac{\omega_2}{2\omega_1}\sqrt{\frac{\gamma_2}{\gamma_1}}[e_{14}]^T$, $\gamma_1 = [e_{14}]^T$, $\omega_1 = [2e_{14}]^T$, $\gamma_2 = [4\cdot 10^{-10}e_3 \quad 8{\cdot}10^{-9}e_3 \quad 4{\cdot}10^{-10}e_8]^T$, $\omega_2 = [2e_{14}]^T$ and $\alpha_m = [5{\cdot}10^{-3}e_6 \quad 5{\cdot}10^{-6}e_8]^T$, where e_i is a $1\times i$ vector of ones. In Fig. 2 the reference trajectory for the position, the orientation and the movement of the joints together with the states are shown. In Fig. 3a the sliding surface σ is shown, in Fig. 4a the thruster forces and joint torques used are shown, and in Fig. 5 the evolution of the gain $k_1(t)$ over time is shown.

From Fig. 2 we can see that the desired trajectories for position, orientation and the joints are tracked very well. This is also supported by Fig. 3, as σ is below 0.07 for the position and orientation and below $5\cdot10^{-4}$ for the joints in absolute value. From Fig. 4 we can see that the forces used is smooth, i.e. no chattering and below $100N$, which is the limit for the thrusters. In Fig. 5 we can see that the gain $k_1(t)$ increases linearly and converges to a suitable value, this fits what we found in Sec. II.

For comparison, in Fig. 3b the sliding surface σ and in Fig. 4b the thruster forces and joint torques are shown, when the GSTA with constant gains is used, with gains $k_1 = [5e_{14}]^T$, $k_2 = [0.02e_{14}]^T$ and $\beta_{\text{GSTA}} = [80e_{14}]^T$. By comparing the sliding surfaces in Fig. 3 we can see that the adaptive GSTA gives considerably smaller sliding surface values than the GSTA with constant gains. By comparing the thruster forces and joint torques in Fig. 4 we can see that when the joints move at 80s (because the AIAUV is moving into operation mode) the adaptive GSTA provides higher thruster forces and joint torques. The rest of the time the thruster forces and joint torques used are similar. This is probably some of the reason why the adaptive GSTA gives a much smaller sliding surface. However, we do also see that the sliding surface is smaller for the adaptive GSTA when the thruster forces and joint torques used are similar. We can therefore conclude that the adaptive GSTA here gives better tracking performance than the GSTA with constant gains.

IV. Conclusions and Future Research

A novel adaptive GSTA is proposed. The proposed approach consists in using dynamically adapted control gains that ensures GFT convergence in the presence of time- and state-dependent perturbations and uncertain control coefficients, such that no conservative upper-bound as to be taken

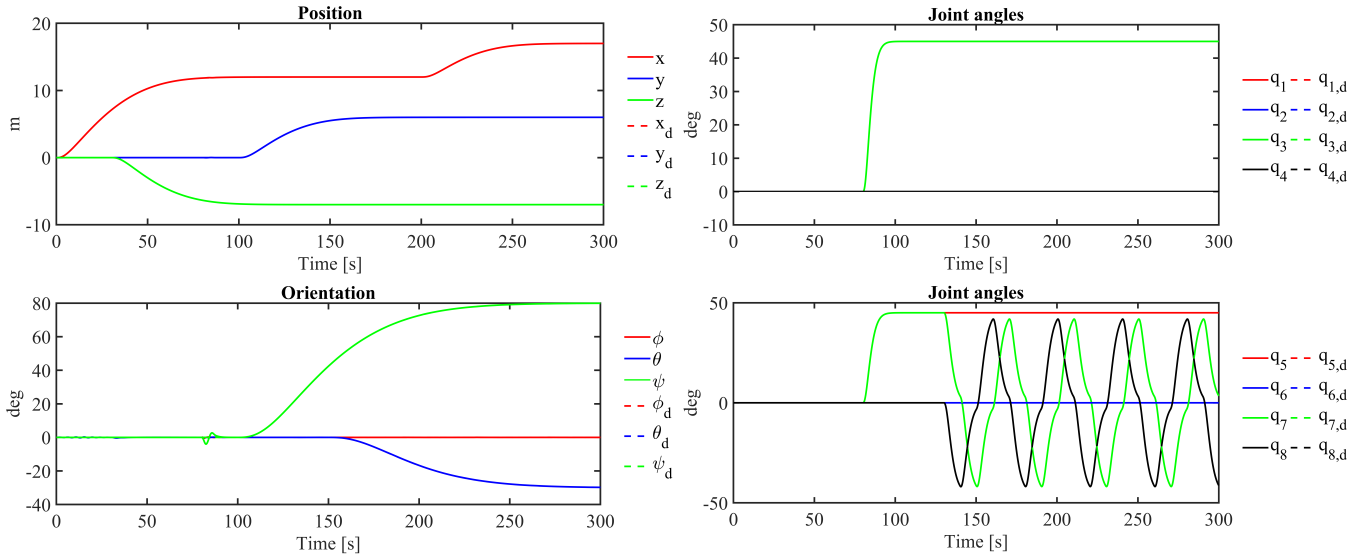

(a) Tracking of position and orientation

(b) Tracking of joint angles

Fig. 2: Tracking results using adaptive GSTA

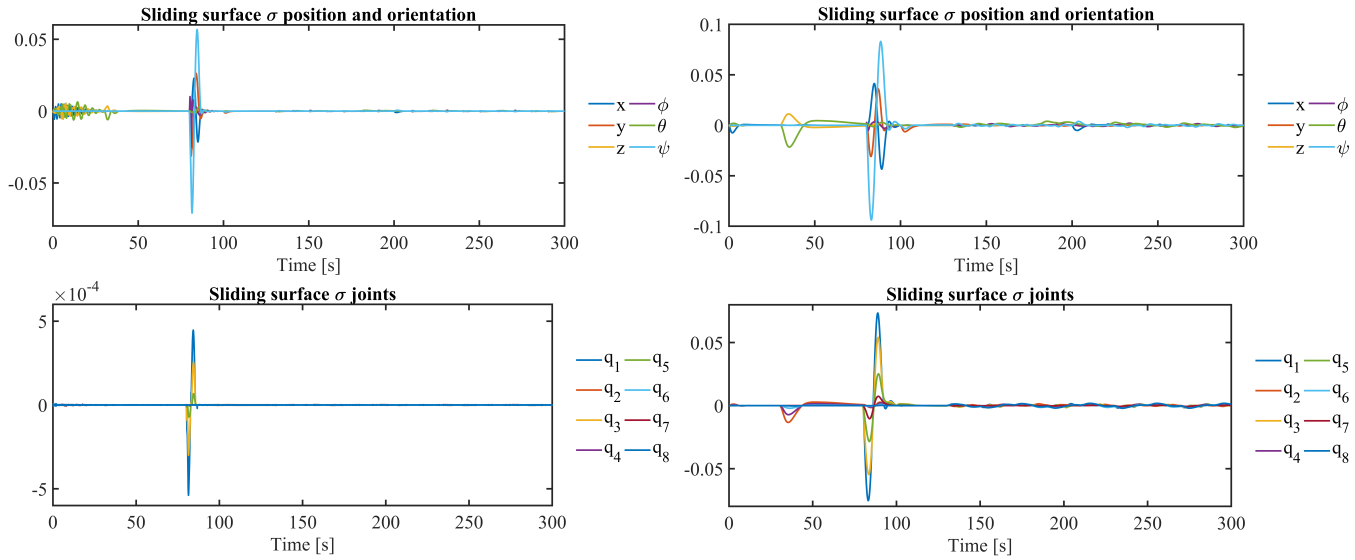

(a) Sliding surface σ using adaptive GSTA

(b) Sliding surface σ using GSTA

Fig. 3: Sliding surface σ

on the uncertainties. It is also shown that the adaptive GSTA makes the tracking errors of the AIAUV converge asymptotically to zero, and a simulation study is performed which shows the effectiveness of the proposed adaptive GSTA. Future work includes experiments to investigate the performance of the control algorithm in practice.

ACKNOWLEDGEMENT

This research was funded by the Research Council of Norway through the Centres of Excellence funding scheme, project No. 223254 NTNU AMOS.

REFERENCES

[1] V. I. Utkin, *Sliding Modes in Control and Optimization*, 1st ed. Berlin, Heidelberg: Springer-Verlag, 1992.

[2] J. A. Burton and A. S. I. Zinober, "Continuous approximation of variable structure control," *International Journal of Systems Science*, vol. 17, no. 6, pp. 875–885, 1986.

[3] J.-J. Slotine and W. Li, *Applied Nonlinear Control,*, 1st ed. Englewood Cliffs, N.J: Prentice-Hall, 1991.

[4] A. Levant, "Higher-order sliding modes, differentiation and output-feedback control," *International Journal of Control*, vol. 76, no. 9-10, pp. 924–941, 2003.

[5] ——, "Homogeneity approach to high-order sliding mode design," *Automatica*, vol. 41, no. 5, pp. 823–830, 2005.

[6] Y. B. Shtessel, I. A. Shkolnikov, and A. Levant, "Smooth second-order sliding modes: Missile guidance application," *Automatica*, vol. 43, no. 8, pp. 1470–1476, 2007.

[7] Y. B. Shtessel, J. A. Moreno, F. Plestan, L. M. Fridman, and A. S. Poznyak, "Super-twisting adaptive sliding mode control: A Lyapunov design," in *Proc. 49th IEEE Conference on Decision and Control*, Atlanta, GA, USA, Dec. 15-17, 2010, pp. 5109–5113.

[8] A. Levant, "Sliding order and sliding accuracy in sliding mode control," *International Journal of Control*, vol. 58, no. 6, pp. 1247–1263, 1993.

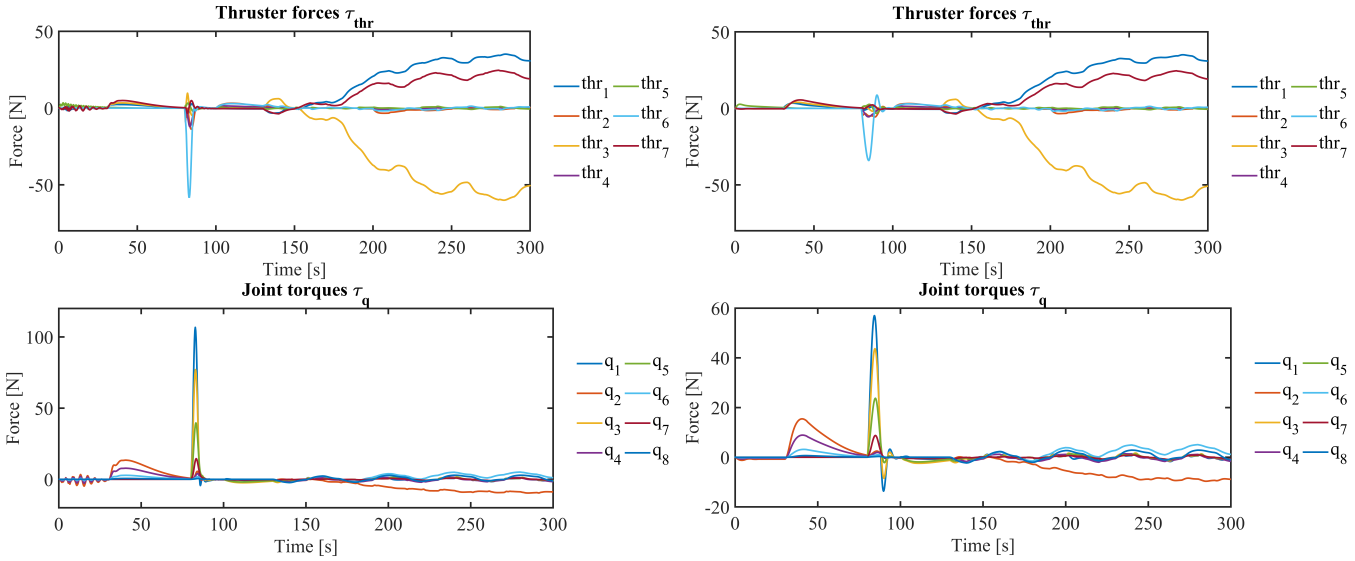

(a) Control input using adaptive GSTA

(b) Control input using GSTA

Fig. 4: Control input

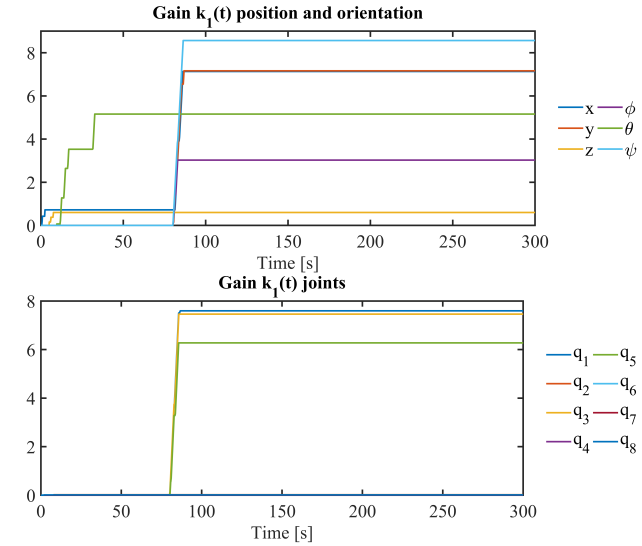

Fig. 5: Evolution of $k_1(t)$ over time

[9] J. A. Moreno, "Lyapunov approach for analysis and design of second order sliding mode algorithms," in *Sliding Modes after the First Decade of the 21st Century: State of the Art*, ser. Lecture Notes in Control and Information Sciences. Berlin, Heidelberg: Springer Berlin Heidelberg, 2012, vol. 412, pp. 113–149.

[10] T. Gonzalez, J. A. Moreno, and L. Fridman, "Variable gain super-twisting sliding mode control," *IEEE Transactions on Automatic Control*, vol. 57, no. 8, pp. 2100–2105, 2012.

[11] E. Guzmn and J. A. Moreno, "Super-twisting observer for second-order systems with time-varying coefficient," *IET Control Theory and Applications*, vol. 9, no. 4, pp. 553–562, 2015.

[12] Y. Shtessel, M. Taleb, and F. Plestan, "A novel adaptive-gain super-twisting sliding mode controller: Methodology and application," *Automatica*, vol. 48, no. 5, pp. 759–769, 2012.

[13] I. Castillo, L. M. Fridman, and J. A. Moreno, "Super-Twisting Algorithm in presence of time and state dependent perturbations," *International Journal of Control*, vol. 91, no. 11, pp. 2535–2548, 2018.

[14] Z. Wang, "Adaptive smooth second-order sliding mode control method with application to missile guidance," *Transactions of the Institute of Measurement and Control*, vol. 39, no. 6, pp. 848–860, 2017.

[15] J. Wei, J. Yuan, and Z. Wang, "Adaptive multivariable generalized super-twisting algorithm based robust coordinated control for a space robot subjected to coupled uncertainties," *Proceedings of the Institution of Mechanical Engineers, Part G: Journal of Aerospace Engineering*, vol. 233, no. 9, pp. 3244–3259, 2019.

[16] J. A. Moreno, "A linear framework for the robust stability analysis of a generalized super-twisting algorithm," in *2009 6th International Conference on Electrical Engineering, Computing Science and Automatic Control*, 2009, pp. 1–6.

[17] J. Guerrero, J. Torres, V. Creuze, and A. Chemori, "Trajectory tracking for autonomous underwater vehicle: An adaptive approach," *Ocean Engineering*, vol. 172, pp. 511–522, 2019.

[18] J. Sverdrup-Thygeson, E. Kelasidi, K. Y. Pettersen, and J. T. Gravdahl, "The Underwater Swimming Manipulator - A Bioinspired Solution for Subsea operations," *IEEE Journal of Oceanic Engineering*, vol. 43, no. 2, pp. 1–16, 2018.

[19] I.-L. G. Borlaug, J. T. Gravdahl, J. Sverdrup-Thygeson, K. Y. Pettersen, and A. Loría, "Trajectory tracking for underwater swimming manipulator using a super twisting algorithm," *Asian Journal of Control*, vol. 21, no. 1, pp. 208–223, 2019.

[20] I.-L. G. Borlaug, K. Y. Pettersen, and J. T. Gravdahl, "Trajectory tracking for an articulated intervention AUV using a super-twisting algorithm in 6DOF," *IFAC PapersOnLine*, vol. 51, no. 29, pp. 311–316, Sep. 10-12, 2018, Proc. 11th IFAC Conference on Control Applications in Marine Systems, Robotics, and Vehicles, Opatija, Croatia.

[21] ——, "Tracking control of an articulated intervention AUV in 6DOF using the generalized super-twisting algorithm," in *Proc. American Control Conference*, Philadelphia, USA, Jul. 10-12 2019, pp. 5705–5712.

[22] ——, "Tracking control of an articulated intervention autonomous underwater vehicle in 6DOF using generalized super-twisting: Theory and experiments," Submitted to IEEE Transactions on Control System Technology, 2019.

[23] ——, "Comparison of two second-order sliding mode control algorithms: Theory and experimental results," Submitted to IEEE Journal of Oceanic Engineering, 2019.

[24] Y. Shtessel, C. Edwards, L. Fridman, and A. Levant, *Sliding Mode Control and Observation*, ser. Control Engineering. New York, NY: Birkhuser, 2014.

[25] G. Antonelli, *Underwater Robots*, 3rd ed., ser. Springer Tracts in Advanced Robotics. Springer International Publishing, 2014, vol. 96.

[26] P. J. From, J. T. Gravdahl, and K. Y. Pettersen, *Vehicle-Manipulator Systems: Modeling for Simulation, Analysis, and Control*, ser. Advances in Industrial Control. London: Springer London, 2014.

[27] T. I. Fossen, *Handbook of Marine Craft Hydrodynamics and Motion Control*. Chichester, UK: John Wiley & Sons, Ltd, 2011.

[28] O. E. Fjellstad and T. I. Fossen, "Singularity-free tracking of unmanned underwater vehicles in 6 DOF," in *Proc. 33rd IEEE Conference on Decision and Control*, Lake Buena Vista, Florida, Dec. 14-16 1994, pp. 1128–1133.

[29] H. M. Schmidt-Didlaukies, A. J. Sørensen, and K. Y. Pettersen, "Modeling of Articulated Underwater Robots for Simulation and Control," in *Proc. 2018 IEEE/OES Autonomous Underwater Vehicles*, Porto, Portugal, Nov. 6-9, 2018.